Supplemental material to this article can be found at:
http://dmd.aspetjournals.org/content/suppl/2022/06/14/dmd.122.000829.DC1
1521-009X/50/8/1106–1118$35.00
DRUG METABOLISM AND DISPOSITION
dx.doi.org/10.1124/dmd.122.000829
Drug Metab Dispos 50:1106–1118, August 2022

The Pharmacokinetics, Metabolism, and Clearance Mechanisms of Abrocitinib, a Selective Janus Kinase Inhibitor, in Humans[S]

Jonathan N. Bauman, Angela C. Doran, Amanda King-Ahmad, Raman Sharma, Gregory S. Walker, Jian Lin, Tsung H. Lin, Jean-Baptiste Telliez, Sakambari Tripathy, Theunis C. Goosen, Christopher Banfield, Bimal K. Malhotra, and Martin E. Dowty

Medicine Design (M.E.D), Inflammation and Immunology (T.H.L., J.-B.T.), and Clinical Pharmacology (C.B.), Pfizer Inc., Cambridge, Massachusetts; Medicine Design (J.N.B., A.C.D., A.K.-A., R.S., G.S.W., J.L., T.C.G.) and Clinical Pharmacology (S.T.), Pfizer Inc., Groton, Connecticut; and Clinical Pharmacology, Pfizer Inc., New York, New York (B.K.M.)

Received January 12, 2022; accepted May 5, 2022

ABSTRACT

Abrocitinib is an oral once-daily Janus kinase 1 selective inhibitor being developed for the treatment of moderate-to-severe atopic dermatitis. This study examined the disposition of abrocitinib in male participants following oral and intravenous administration using accelerator mass spectroscopy methodology to estimate pharmacokinetic parameters and characterize metabolite (M) profiles. The results indicated abrocitinib had a systemic clearance of 64.2 L/h, a steady-state volume of distribution of 100 L, extent of absorption >90%, time to maximum plasma concentration of ~0.5 hours, and absolute oral bioavailability of 60%. The half-life of both abrocitinib and total radioactivity was similar, with no indication of metabolite accumulation. Abrocitinib was the main circulating drug species in plasma (~26%), with 3 major monohydroxylated metabolites (M1, M2, and M4) at >10%. Oxidative metabolism was the primary route of elimination for abrocitinib, with the greatest disposition of radioactivity shown in the urine (~85%). In vitro phenotyping indicated abrocitinib cytochrome P450 fraction of metabolism assignments of 0.53 for CYP2C19, 0.30 for CYP2C9, 0.11 for CYP3A4, and ~0.06 for CYP2B6. The principal systemic metabolites M1, M2, and M4 were primarily cleared renally. Abrocitinib, M1, and M2 showed pharmacology with similar Janus kinase 1 selectivity, whereas M4 was inactive.

SIGNIFICANCE STATEMENT

This study provides a detailed understanding of the disposition and metabolism of abrocitinib, a Janus kinase inhibitor for atopic dermatitis, in humans, as well as characterization of clearance pathways and pharmacokinetics of abrocitinib and its metabolites.

Introduction

Abrocitinib (PF-04965842) is a selective small molecule Janus kinase (JAK)-1 inhibitor under development at daily doses of 200 and 100 mg to treat moderate-to-severe atopic dermatitis (Gooderham et al., 2019;Silverberg et al., 2020; Simpson et al., 2020; Bieber et al., 2021). Selective inhibition of cytokines by abrocitinib that signal through JAK1 dependent pairs [i.e., JAK1/JAK2, JAK1/JAK3, and JAK1/tyrosine kinase (TYK) 2] includes interleukin (IL)-4, IL-13, and other cytokines (e.g., IL-31, IL-22, and thymic stromal lymphopoietin) involved in the pathogenesis of atopic dermatitis and pruritus (Trier and Kim, 2018) while sparing non-JAK1 pairs such as JAK2/JAK2 inhibition and thereby minimizing the risk for neutropenia and anemia (Akada et al., 2014).

Abrocitinib is a weak base of molecular mass 323.4 with measured logP of 1.7 and pK_a of 5.2 (data on file). Abrocitinib showed high in vitro permeability in Madin-Darby canine kidney cells at 16×10^{-6} cm/s. Aqueous solubility was pH dependent at ~8 mg/mL at pH ~1 and ~35 μg/mL at pH ~8. Abrocitinib pharmacokinetics have been investigated in healthy volunteers (Peeva et al., 2018). Abrocitinib was absorbed rapidly following single doses of 3–200 mg [the median time that plasma C_{max} occurred (T_{max}) was <1 hour] and more slowly at higher doses of 400 and 800 mg (median T_{max} 1.5–4.0 hours), indicating some delayed absorption at higher doses. Plasma C_{max} increased proportionally from 3 to 800 mg; the area under concentration-time curve extrapolated to infinity (AUC_{inf}) was greater than proportional with doses of 400 and 800 mg. Multiple dose pharmacokinetics

This was a Pfizer-sponsored study, and the work received no external funding.
All authors are full-time employees and shareholders of Pfizer Inc. The authors have no conflicts of interest that are directly relevant to this study.
dx.doi.org/10.1124/dmd.122.000829.
[S] This article has supplemental material available at dmd.aspetjournals.org.

ABBREVIATIONS: ADME, absorption, distribution, metabolism, excretion; AMS, accelerator mass spectroscopy; AUC, area under the curve; AUC_{inf}, area under the concentration-time curve from time 0 to infinity; B/P, blood to plasma ratio; CL_{int}, intrinsic clearance; $CL_{int,app}$, apparent intrinsic clearance; $CL_{int,app,sc}$, scaled in vivo apparent intrinsic clearance; COSY, homonuclear correlation spectroscopy; EM, extensive metabolizer; f_af_g, fraction absorbed × fraction surviving gut metabolism; f_{CL}, fraction of abrocitinib clearance represented by metabolite x determined in radiolabeled human hepatocyte experiments; f_m, fraction of metabolism; f_u, fraction unbound in plasma; HLM, human liver microsome; HMBC, heteronuclear multiple bond correlation spectroscopy; HPLC, high-performance liquid chromatography; hWB, human whole blood; IFN, interferon; IL, interleukin; JAK, Janus kinase; *Ki*, inhibition constant for substrates exhibiting substrate inhibition kinetics; *Km*, apparent substrate concentration at half-maximal velocity; LC-MS, liquid chromatography–mass spectrometry; LC-MS/MS, liquid chromatography–tandem mass spectrometry; M, metabolite; P450, cytochrome P450; PPP, 2-phenyl-2-(1-piperdinyl)propane; QC, quality control; *S*, substrate concentration; STAT, signal transducer and activator of transcription; $t_{1/2}$, half-life; T_{max}, time to maximum plasma concentration; TYK, tyrosine kinase; UHPLC, ultra-high-performance liquid chromatography.

showed steady state was reached by day 4 with an observed accumulation ratio of 1.3:1.5 with once-daily dosing between 30 and 200 mg, and plasma half-life ranged between approximately 2 and 4 hours. Renal clearance of abrocitinib was estimated to between 0.59 to 0.67 L/h (Peeva et al., 2018).

Examining human radiolabeled absorption, distribution, metabolism, and excretion (ADME) provides a comprehensive profile of the disposition of a drug. Recent application of accelerator mass spectrometry (AMS) analytical methodology to human ADME studies has been an important advancement in study design as this enables administration of up to 1000-fold lower doses of carbon-14 compared with traditional methods of study (Spracklin et al., 2020). Using microtracer of carbon-14 (0.1–1 μCi) administration, more informative ADME studies that include two-period fixed sequence oral (period A) and intravenous (period B) designs can be performed; these studies allow the determination of additional drug parameters including systemic clearance, volume of distribution, gut availability, and absolute bioavailability. In addition, the low level of radioactivity eliminates the need for the prerequisite quantitative whole-body autoradiography rat study to estimate dosimetry or the need to run nonclinical safety studies with an intravenous formulation since the microtracer is adequately supported by oral toxicology studies. An important design element of the microtracer intravenous period is the administration of a clinically relevant nonlabeled dose of the drug, followed by the administration of the intravenous microtracer of ^{14}C-drug at approximately T_{max} to reflect an appropriate total mass of drug in the body and allow scaling of the intravenous pharmacokinetic parameters to a therapeutic dose (Spracklin et al., 2020).

The objectives of the present fixed-dose crossover oral and intravenous study were to investigate the disposition, mass balance, and metabolic profiles of a therapeutic oral dose of 200 mg abrocitinib in healthy participants as well as determine its systemic clearance, volume of distribution, gut availability, and absolute bioavailability. In addition, metabolic clearance mechanisms of abrocitinib were investigated with in vitro hepatic systems, and in vitro pharmacology of both abrocitinib and primary circulating metabolites was assessed in human whole-cell assays.

Materials and Methods

Materials and Reagents

Abrocitinib (PF-04965842), its deuterated standard (PF-06651703), and metabolites (M)-1 (PF-06471658), M2 (PF-07055087), M3 (PF-07055090), M4 (PF-07054874), M5 (PF-07054926), M6 (PF-07095462), M7 (PF-06737821), and 2-phenyl-2-(1-piperdinyl) propane (PPP) were synthesized at Pfizer Inc. (Groton, CT). ^{14}C-abrocitinib (^{14}C label on the 2-position of the carbon of the pyrimidine ring) was synthesized by Perkin Elmer Inc. (Boston, MA), with radiochemical purity of 98.3% and specific radioactivity of 6.31 μCi/mg. Analytical chemicals of analytical grade or better were obtained from Fischer Scientific (Waltham, MA). $MgCl_2$, NADPH, diclofenac, furafylline, tienilic acid, esomeprazole, quinidine, aminobenzotriazole, 1 M potassium phosphate dibasic solution, 1 M potassium phosphate monobasic solution, sodium bicarbonate, and DMSO were purchased from Sigma Aldrich (St. Louis, MO). Troleandomycin was ordered from Fischer Scientific (Waltham, MA), and gemfibrozil acyl glucuronide was synthesized at Wuxi App Tec (Shanghai, China). HPLC solvents included ammonium acetate, acetonitrile, methanol, and formic acid from Biosolve (Valkenswaard, Netherlands); trifluoracetic acid from Sigma Aldrich (Amsterdam, Netherlands); isopropyl amine from iPAm, Merck (Amsterdam, Netherlands); 2 mM ammonium acetate/methanol/acetonitrile (95/2.5/2.5% v/v) from Brand-Nu Laboratories (Meriden, CT); and methanol, acetonitrile, and water from J.T. Baker (Avantor, Radnor, PA). Cell culture medium included Williams E media (GIBCO-BRL custom formula Lot# 1701813) and HEPES (Lonza, Switzerland). Pooled human liver microsomes (HLM) [HLM103, 20.0 mg of protein per ml, 0.31 nmol of cytochrome P450 (P450) per mg of protein] were prepared and characterized by Sekisui Xenotech (Kansas City, KS) from 50 individual human donors of both sexes. Cryopreserved human hepatocytes (lot DCM) were prepared and characterized by Bioreclamation IVT (Baltimore, MD) from 10 individual donors of both sexes.

Clinical Study and Sample Collection

This study was a phase I, open-label, nonrandomized, 2-period, fixed sequence study conducted at PRA-EDS International (Groningen, Netherlands). Six healthy male participants (1 Hispanic/5 non-Hispanic), 22–28 years of age, with a mean body weight of 83.1 kg and body mass index of 24.4 kg/m^2 were enrolled. Participants were genotyped for CYP2C19 and 2C9 with commercially available TaqMan assays and analyzed on a QuantStudio 12K Flex Real-Time PCR System. Each participant received 2 dose regimens in periods A and B (14 days following period A) following an overnight fast. Period A was an oral solution dose of 200 mg abrocitinib and 80 μg ^{14}C-abrocitinib. Plasma samples were collected before dosing and from 0.25 to 96 hours after dose. Urine and feces were collected prior to dose and up to 240 hours following dose (excreta collection continued until at least 90% of administered dose was recovered or less than 1% was recovered from excreta from 2 consecutive days). Period A samples were analyzed for total ^{14}C and metabolite profiling. Period B was an oral solution dose of 200 mg abrocitinib followed by a 100 μg ^{14}C-abrocitinib intravenous approximately 1 hour later (T_{max}). Plasma samples were collected before dose and at various times postdose and analyzed for total ^{14}C, ^{14}C-abrocitinib (0.083–95 hours postintravenous dose), and abrocitinib (0.25–96 hours following oral dose) concentrations. Urine was collected before dose and up to 143 hours postintravenous dose and analyzed for total ^{14}C radioactivity. Feces were not collected in period B based on the observation that <10% of dose was recovered in feces in period A. The final protocol and informed consent documentation were reviewed and approved by the Independent Ethics Committee at the investigational center participating in the study. This study was conducted in compliance with the ethical principles originating in or derived from the Declaration of Helsinki and in compliance with all International Council for Harmonization Good Clinical Practice Guidelines.

Radiochemical Analysis

Analyses of total ^{14}C radioactivity in plasma, urine, and feces homogenate were conducted at TNO (Microbiology and Systems Biology, Zeist, Netherlands) using ^{14}C detection by AMS. AMS analysis was performed on a 1MV multielement AMS, model 4110 Bo, High Voltage Engineering (software: AMS 155). Low-level scintillation counting was performed on a Quantulus 1220 (software WinQ version 1.2). Aliquots of plasma (5 μL), urine (15 μL, diluted or undiluted) or feces homogenate [homogenized at the PRA Health Sciences Bioanalytical Laboratory (Drenthe, Netherlands), 30 mg, diluted or undiluted] was transferred to tinfoil cups. The samples were dried under a stream of nitrogen and subsequently placed in the elemental analyzer (Vario Micro; Elementar, Langenselbold, Germany), which acted as autosampler and CO_2 combustion device for the AMS (van Duijn et al., 2014). The natural background ^{14}C/^{12}C level, measured in predose samples of each matrix, was subtracted to obtain the amount of ^{14}C abrocitinib-related ^{14}C. ^{14}C/^{12}C isotope ratios of the samples were converted to mBq/mL for plasma and urine samples, whereas the homogenized feces samples data were converted into mBq/g. The total ^{14}C radioactivity concentrations in urine and feces were further converted to percentage of dose recovered in urine and feces based upon the radioactivity dose administered to each participant. A reference standard ANU sucrose-8542 with a certificated ^{14}C/^{12}C isotope ratio was used as system suitability sample. In each batch, the measured ^{14}C/^{12}C ratio deviated <15% from the certified ratio. Plasma standard samples were included in each analysis as AMS quality control (QC) samples with a minimum of 3 replicates. The samples were prepared by spiking blank pooled plasma with a known amount of ^{14}C (from ^{14}C-paracetamol). The ^{14}C/^{12}C ratios were determined by AMS and found to deviate no more than 15% from the nominal value. In addition, the CV was also <15%.

Metabolite Profiling in Plasma, Urine, and Feces

Sample Preparation. To profile circulating metabolites, plasma samples from each individual at 0–12 hours postdose, which covered >97% of the total radioactivity area under the curve (AUC), were pooled according to the method of Hamilton et al. (1981). The pre- and postdose pools were prepared using equal volumes from each participant. The pooled plasma (100 μL) was diluted with acetonitrile (500 μL), vortexed for 1 minute, and centrifuged (14,000*g*, 5 minutes,

10°C). After centrifugation, 500 μL supernatant was removed and dried under a stream of nitrogen. The residue was dissolved in 2 mM ammonium acetate/acetonitirile/methanol (80%:10%:10% v:v:v), vortexed for 30 seconds, and centrifuged (1000*g*, 1 minute, room temperature). Urine samples collected from each participant from 0 to 12 hours following dosing represented 96% of the excreted radioactivity. A predose pool was prepared by mixing equal volumes of each predose sample. An equal volume from each individual was pooled, 50 μL of urine sample, 700 μL 2 mM ammonium acetate/acetonitirile/methanol (80%:10%:10% v:v:v) was added, vortexed for 1 minute, and centrifuged (1000*g*, 1 minute, room temperature). Individual fecal homogenate pools accounting for 97% of the total dose collected from feces were prepared for each participant by combining proportional amounts of the sample collected over each time period (48–144 hours, 24–96 hours, 24–72 hours, 48–168 hours, 0–48 hours, and 0–72 hours, respectively). An equal amount from each individual participant pool was then combined into a master pool. A pooled predose sample was prepared by taking equal aliquots per participant. To a 100 mg of feces homogenate sample, 500 μL acetonitrile was added, equilibrated for 5 minutes, and vortexed for 1 minute. The sample was centrifuged (14,000*g*, 5 minutes, 10°C), 500 μL supernatant was removed, and a second extraction was performed using the same methods. The residue was dissolved in 2 mM ammonium acetate/acetonitirile/methanol (80%:10%:10% v:v:v), vortexed for 30 seconds, and centrifuged (1000*g*, 1 minute, room temperature). Sample extraction and liquid chromatography–mass spectrometry (LC-MS) profiling column recoveries were all greater than 89%.

Metabolite Profiling Ultra-High-Performance Liquid Chromatography Methods. Pooled urine and extracts from pooled plasma and homogenized feces were profiled using a high-resolution liquid chromatography–tandem mass spectrometry (LC-MS/MS) method described in Supplemental Table 1. After the column, the eluent was split: 1) part of the flow was used to generate on-line high-resolution mass spectrometry (MS) [and/or the data-dependent mass spectrometry/mass spectrometry (MS/MS) spectrum], and 2) the other part of the flow was collected for off-line AMS analysis. For each chromatogram, a total of 154 fractions were collected (0–14 minutes, 6-second fractions; 14–28 minutes, 1-minute fractions).

AMS Analysis. To each fraction from 0–14 minutes, additional carbon-12 was added (paracetamol in methanol), and the whole fraction was transferred to a tinfoil cup, dried under a stream of nitrogen, and subsequently placed in the elemental analyzer, which acted as autosampler and combustion device for the AMS. To each fraction from 14–28 minutes, additional carbon-12 was added to obtain a suitable amount of carbon for AMS analysis. An aliquot of 60 μL was transferred to a tinfoil cup, dried under a stream of nitrogen, and subsequently placed in the elemental analyzer, which acted as autosampler and combustion device for the AMS.

Metabolite Identification. The Q Exactive mass spectrometer operated in the positive electrospray ionization mode. The heated electrospray ion source voltage was 3.0 kV. The heated capillary temperature was 350°C. Auxiliary and spare gases were set to 20 and 0 units, respectively. The scan-event cycle consisted of a full-scan mass spectrum (100–1000 m/z) at a resolving power of 35,000, and the corresponding data-dependent tandem mass spectrometry scans were acquired at a resolving power of 35,000. Accurate mass measurements were performed using external calibration. A reference list of known metabolites of abrocitinib and their expected molecular ions was added to an inclusion list to prioritize those ions during data acquisition. Postacquisition searching of LC-MS data for molecular ions representing possible metabolites of ^{14}C abrocitinib was performed manually. In addition, the LC-MS data associated with every radiochromatographic peak was also interrogated. LC-MS peaks identified to be possible metabolites, based on the molecular ions, were compared against blank samples. In cases where the signal strength was of sufficient intensity to trigger data-dependent tandem mass spectrometry, the subsequent fragment spectra were examined to further confirm the identity and structure of possible metabolites. In addition, LC-MS chromatograms were compared directly against the appropriate predose matrix chromatogram to identify additional metabolite peaks.

Chiral Separation of Metabolites M2 and M3. Plasma, urine, and feces homogenate extracts were injected in triplicate using the UHPLC system described above (Supplemental Table 1), and the fraction containing both enantiomers was collected. For each matrix, these 3 fractions (from the triplicate injections per matrix) were pooled and dried under a stream of nitrogen. The dried fractions were reconstituted in 200 μL mobile phase [0.1% trifluoroacetic acid, 0.1% isopropylamine in acetonitrile/methanol (90%:10% v:v)]. The reconstituted fractions were injected on the UHPLC where the chromatography was performed using a ChiralPAK ZWIX(-) (4 × 150 mm, 3 μm, Diacel, Chiral Technologies, Inc., West Chester, PA). An isocratic flow rate of 0.25 mL/min was maintained throughout the analysis. For each matrix, a duplicate injection of 25 μL was performed. After the column, the eluent was fraction collected for off-line AMS analysis.

Isolation of Metabolites M6 and M7. Approximately 30 mL of 0- to 24-hour–pooled human urine was centrifuged at 1800*g* for 20 minutes and the supernatant applied to a Bond Elut C-18 SPE cartridge (10 gm, Agilent Technologies, Santa Clara, CA) equilibrated in 5% methanol in water at a flow rate of 2.0 mL/min. The cartridge was successively eluted with 50 mL of 10 mM ammonium acetate in water containing varying percentages of 1:1 methanol/acetonitrile (2.5%, 5%, 10%, 15%, 20%, 25%, 30%, and 2.5%). Fifty microliters of the flow through and each eluate were analyzed by LC-MS/MS (Supplemental Table 2) to determine which fractions contained metabolites M6 and M7. Eluates rich in M6 and M7 were evaporated to near dryness in a vacuum centrifuge at room temperature. Residues were redissolved in 0.1% formic acid in 1:1 methanol/acetonitrile (97.5%:2.5% v:v), and 5-mL aliquots were fractionated using the LC-MS/MS method shown in Supplemental Table 3. One-minute fractions were collected, and 10 μL of fractions between 9.0 and 36 minutes were analyzed by LC-MS/MS for presence of M6 and M7 metabolites (Supplemental Table 4). Fractions rich in M6 and M7 were pooled and evaporated to dryness in a vacuum centrifuge at room temperature. The residues were redissolved in 1.0 mL 10 mM ammonium acetate/methanol/acetonitrile (97.5%:1.25%:1.25% v:v:v) and purified using the LC-MS/MS method shown in Supplemental Table 5. One-minute fractions were collected, and 10 μL of fractions between 4.0 minutes and 32 minutes were analyzed by LC-MS/MS (Supplemental Table 4) for presence of m/z 354 (M7) and m/z 370 (M6) metabolites. Fractions containing metabolites were then pooled and evaporated to dryness for NMR analysis.

Nuclear Magnetic Resonance Characterization of Metabolite M6 and M7. All samples were dissolved in 0.05 mL of DMSO-d6 "100%" (Cambridge Isotope Laboratories, Andover, MA) and placed in a 1.7 mm NMR tube in a dry argon atmosphere. ^{1}H and ^{13}C spectra were referenced using residual DMSO-d6 (2.50 ppm relative to tetramethylsilane, $\delta = 0.00$, 13C $\delta = 39.50$ ppm relative to tetramethylsilane, $\delta = 0.00$). NMR spectra were recorded on a Bruker Avance 600 MHz (Bruker BioSpin Corporation, Billerica, MA) controlled by Topspin V3.1 and equipped with a 1.7 mm TCI Cryo probe. One dimensional spectra were recorded using a sweep width of 10,000 Hz and a total recycle time of 7 second. The resulting time-averaged free induction decays were transformed using an exponential line broadening of 1.0 Hz to enhance signal to noise. The two dimensional data were recorded using the standard pulse sequences provided by Bruker. At minimum, a 1K × 128 data matrix was acquired using a minimum of 2 scans and 16 dummy scans with a spectral width of 10,000 Hz in the *f2* dimension. The data were zero-filled to at least 1K data point.

Abrocitinib Quantification

Plasma samples from period B were analyzed for abrocitinib concentration at WuXi AppTec (Shanghai, China) with a validated LC-MS/MS method. Abrocitinib and internal standard PF-06651703 (deuterated abrocitinib) were extracted from 75 μL human plasma using liquid-liquid extraction with ethyl acetate, and extracts were analyzed with the LC-MS/MS method shown in Supplemental Table 6. The calibration range was 1.00–2000 ng/mL, and the QC concentrations were 3.00, 60.0, 1000, and 1600 ng/mL. The interday assay accuracy ranged from –4.8% to 0.0%, and the between-day precision was ≤7.8%.

Plasma samples from period B were analyzed for ^{14}C-abrocitinib concentration at TNO (Microbiology and Systems Biology, Ziest, Netherlands) using a qualified analytical method. Protein precipitation of 100 μL plasma was performed using 3:1 acetonitrile/plasma followed by centrifugation, drying under a stream of nitrogen, and reconstitution with 80:10:10 2 mM ammonium acetate/acetonitrile/methanol. Samples were analyzed by LC-MS/MS methods (Supplemental Table 1) with AMS detection (1MV multielement AMS model 4110 Bo, High Voltage Engineering) The calibration range was 0.50–100 mBq/mL, and QC concentrations were 1.50, 20.0, 75.0, and 200 mBq/mL. The interday assay accuracy ranged from –10.9% to –3.0%, and the between-day precision was ≤3.7%.

In Vitro P450 Assignment

The experimental conditions used in vitro were confirmed to yield linear reaction velocities as determined from preliminary range-finding experiments.

In Vitro Hepatocyte Fractional Metabolism. The reaction phenotyping experiment was conducted using ^{14}C abrocitinib (1 μM) incubated in pooled human cryopreserved hepatocytes at 0.75 million cells per mL in William's E Medium at 37°C in 5% CO_2/95% air and 85% relative humidity for 30 minutes. Aliquots were quenched into acetonitrile (1:4, v/v) and centrifuged (1860*g*) for 5 minutes, and the supernatant was transferred to clean 15 mL conical glass tubes. The supernatants were dried in a Genevac (Genevac Inc, Valley Cottage, NY) evaporative centrifuge at 37°C, and the resulting residues were reconstituted in 100 μL of 2 mM ammonium acetate/acetonitrile/methanol (95%:2.5%:2.5% v:v:v).

Sample bioanalysis was performed using the LC-MS/MS method shown in Supplemental Table 7. Postcolumn, the eluent was split: 1) part of the flow was used to generate on-line high-resolution MS (and/or data-dependent MS/MS) spectrum, and 2) the other part of the flow was diverted to the fraction collector. Fractions were collected in 6-second intervals into Lumaplate-96 well plates (PerkinElmer, Waltham, MA) and dried in a Genevac evaporative centrifuge at 37°C. Plates were then placed in a PerkinElmer MicroBeta2 counter and each well counted for total ^{14}C for 5 minutes. The results were used to generate a reconstructed radiochromatogram.

Enzyme Kinetics. Experiments for the determination of enzyme kinetic parameters were conducted in human liver microsomes. Abrocitinib (0.1–1000 μM) was incubated in 100 mM potassium phosphate buffer (pH 7.4) containing 3 mM $MgCl_2$ and 0.3 mg/mL microsomal protein HLM-103 at 37°C. Reactions were initiated with NADPH (1.2 mM) immediately followed by substrate and terminated after 15 minutes by quenching aliquots of the incubation mixture with acetonitrile-containing internal standard (Diclofenac, 10 ng/mL). Samples were centrifuged (1700*g*) for 10 minutes, and 100 μL of supernatant was transferred to a 96 deep-well plate. The supernatants were dried down under a stream of nitrogen and reconstituted in 100 μL of 90% water/10% acetonitrile. Incubations for enzyme kinetic determination were conducted in triplicate.

P450 Chemical Inhibition. The P450-selective chemical inhibition experiment was conducted using abrocitinib (10 μM), pooled human hepatocytes, and chemical inactivators of P450s 1A2, 2B6, 2C8, 2C9, 2C19, 2D6, 3A, and pan-P450 in a 96-well plate. Hepatocytes (120 μL) at 0.75 million cells per mL in Williams E media were preincubated with inhibitors for 15 or 30 minutes prior to initiating the reactions by the addition of abrocitinib. Incubations containing 100 μM gemfibrozil glucuronide (CYP2C8), 15 μM tienilic acid (CYP2C9), and 1 mM 1-aminobenzotriazole (pan-P450) were preincubated for 30 minutes, and 10 μM furafylline (CYP1A2), 5 μM PPP (CYP2B6), 5 μM esomeprazole (CYP2C19), 2 μM CYP3cide (CYP3A4), and 25 μM troleandomycin (CYP3A4/5) were preincubated for 15 minutes with human hepatocytes to achieve complete inactivation of respective P450 isoforms (Walsky and Obach, 2007; Yang et al., 2016). Quinidine (10 μM) was used as a competitive inhibitor (CYP2D6) without preincubation prior to the addition of abrocitinib. Incubations of abrocitinib were conducted at 37°C in 5% CO_2/95% air and 75% relative humidity for 30 minutes. Aliquots were collected into acetonitrile-containing internal standards to quench the reaction. Quenched samples were centrifuged (1700*g*) for 10 minutes, and 150 μL of supernatant was transferred to a 96 deep-well plate. The supernatants were dried under a stream of nitrogen and reconstituted in 100 μL of 10% acetonitrile/90% water. Selective chemical inhibition experiments were conducted in triplicate.

Enzyme Kinetics and Chemical Inhibition Bioanalysis. Sample bioanalysis was performed using the LC-MS/MS method shown in Supplemental Table 8. Integration and quantitation of metabolites and internal standard molecule peak areas were performed using Analyst version 1.6.2 (AB Sciex) to derive the analyte to internal standard peak area ratios. Standard curves for the quantitation of metabolite concentrations were prepared from plots of area ratio versus concentration and analyzed using a linear regression with either 1/x or 1/x 2 weighting.

Fractional Clearance in Human Hepatocytes. To determine the fractional contributions of metabolic pathways of ^{14}C-abrocitinib, radioactivity counts for fractions were plotted against time to reconstruct liquid chromatography chromatograms, which were then aligned and assessed against MS spectral data for agreement. The sum of radioactive counts associated with an individual chromatographic peak was determined and compared with the total radioactivity recovered to derive the percentage of total radioactivity using the 30-minute time point. The contribution of a single metabolic pathway (represented by an individual metabolite plus any secondary metabolites deriving from it) was calculated as the response of the individual metabolite divided by the total metabolism of abrocitinib.

Enzyme Kinetics in Human Liver Microsomes. Substrate concentration (*S*) and velocity (*V*) data were fitted to the appropriate enzyme kinetic model by nonlinear least-squares regression analysis (SigmaPlot version 13; Systat Software, Inc., San Jose, CA or GraphPad version 6.03; GraphPad Software Inc., La Jolla, CA) to derive the apparent enzyme kinetic parameters using the Michaelis-Menten model (eq. 1) and the substrate inhibition model (eq. 2).

$$V = \frac{V_{\max} \times S}{K_m + S} \tag{1}$$

$$V = \frac{V_{\max} \times S}{K_m + S \times (1 + S/Ki)} \tag{2}$$

where V_{max} is the maximal velocity, K_m or S_{50} is the substrate concentration at half-maximal velocity, and *Ki* is an inhibition constant. The best fit was based on a number of criteria, including visual inspection of the data plots (Michaelis-Menten and Eadie-Hofstee), distribution of the residuals, size of the sum of the squared residuals, and the standard error of the estimates. Selection of models other than Michaelis-Menten was based on the F-test ($P < 0.05$) or the Akaike Information Criterion.

In vitro apparent intrinsic clearance (CL_{int}) values were calculated using eq. 3:

$$CL_{\text{int}} = \frac{V_{\max}}{K_m} \tag{3}$$

CL_{int} data were also calculated from rate of product formation (*V*) obtained at *S* below the apparent K_m [$(S) < K_m$], in which cases eq. 1 was rearranged to $CL_{int} = V/[S]$.

In vitro apparent intrinsic clearance ($CL_{int,app}$) and scaled in vivo apparent intrinsic clearance ($CL_{int,app,sc}$) values for M1, M2/M3, and M4 were calculated using the following equations:

$$CL_{int,app(HLM)} = \frac{V_{max}}{K_m} \tag{4}$$

$$CL_{int,app,sc(HLM)} = CL_{int,app(HLM)} \times 45\ mg\ protein/gram\ liver \times 21\ g\ liver/kg\ body\ weight \tag{5}$$

Selective P450 Chemical Inhibition in Human Hepatocytes. To determine the contribution of each P450 isoform to abrocitinib metabolism in human hepatocytes, the metabolite formation rates were calculated by dividing the metabolite concentration by incubation time and protein concentration. The effect of P450 selective chemical inhibitors on the formation rate of each metabolite was calculated using the following formula:

$$\%Inhibition(unscaled) = \left(1 - \frac{v_{inh}}{v_{ctrl}}\right) \times 100 \tag{6}$$

wherein v^{inh} is the rate of formation in the presence of inhibitor and v^{ctrl} is the rate of metabolite formation in the control human hepatocyte incubation. To determine the contribution of each P450 isoform for the metabolites without standard, the analyte-to-internal-standard-area ratio was used. When the combined inhibitor effects on a metabolic pathway totaled more than 100%, the percentage inhibition values for that pathway were normalized to 100%. The fraction of abrocitinib metabolism represented by a single metabolite *x* and specific P450 isoform *z* ($f_{mMx,P450z}$) was calculated using the following equation:

$$f_{mMxP450z} = \frac{\%\ inhibition}{100} \times f_{CL} \tag{7}$$

where % inhibition is the scaled inhibition of metabolite *x* by a P450-specific inhibitor *z*, and f^{CL} is the fraction of abrocitinib clearance represented by metabolite *x* determined in radiolabeled human hepatocyte experiments.

A statistical analysis was conducted comparing the metabolite formation rates in the presence of inhibitor versus control incubations to confirm

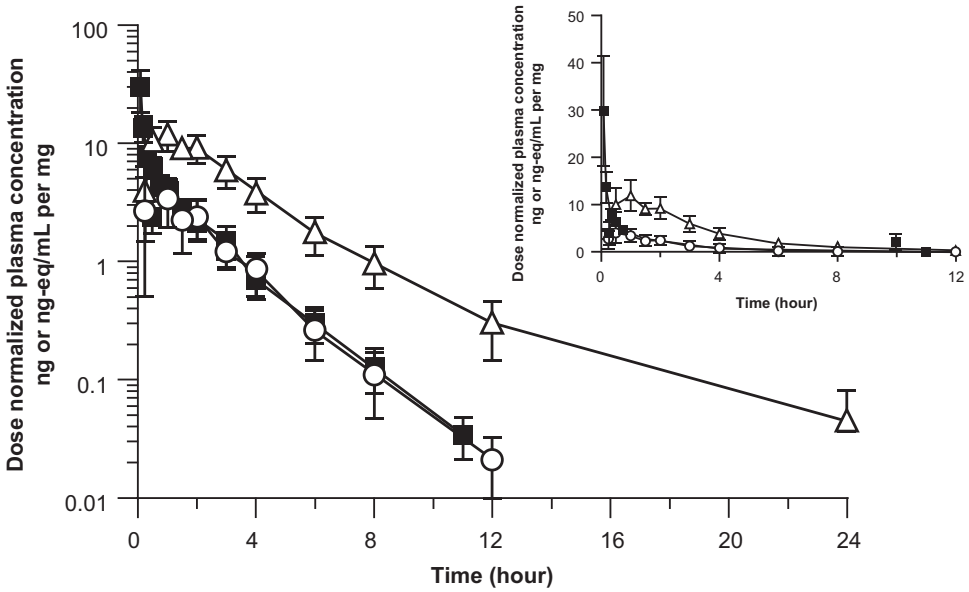

Fig. 1. Dose-normalized log mean (plus or minus standard deviation) plasma concentration-time profiles (linear inset) for abrocitinib (○ = 200 mg oral and ■ = 100 μg i.v.) and total radioactivity (Δ = 80 μg oral) following single dose administration. ng-eq, nanogram-equivalent.

significance. A one-way analysis of variance analysis with a Dunnett's Test for multiple comparisons was applied to the triplicate values from inhibited and control conditions.

In Vitro Pharmacology

The potency of abrocitinib and its metabolites against the four JAK isoforms, JAK1, JAK2, JAK3, and TYK2, was measured in terms of IC_{50} as previously reported (Dowty et al., 2019). In addition, the potency of abrocitinib and its metabolites to inhibit the ability of various cytokines to induce signal transducer and activator of transcription (STAT) phosphorylation in human whole blood, human keratinocytes, or human acute monocytic leukemia (THP-1) cells was assessed as previously reported (Dowty et al., 2019). More methodology details are provided in the Supplemental Methods.

TABLE 1

Mean pharmacokinetic parameters for abrocitinib following intravenous and oral administration

Plasma Pharmacokinetics		
Parameter	^{14}C-Abrocitinib,[a]Intravenous	Abrocitinib, Oral
Period	B	B
Dose, mg	0.1	200
Body weight, kg (S.D.)	83.1 (13.7)	83.1 (13.7)
AUC_{inf}, ng* h/mL	1.56 (15)	1850 (35)
C_{max}, ng/mL		778 (45)
T_{max}, h (range)		0.50 (0.5–2.0)
$t_{1/2}$, h (S.D.)	1.45 (0.08)	1.52 (0.09)
CL, L/h	64.2 (14)	
V_{ss}, L	100 (19)	
%F[b] (90% CI)		59.8 (45.9–77.8)

Urine Pharmacokinetics		
Parameter	Total ^{14}C PO	Total ^{14}C Intravenous
Period	A	B
% of ^{14}C dose in urine	85.1 (7)	93.3 (1)
$\%f_af_g$[c]	91.3	

Plasma pharmacokinetics were assessed during Period B using noncompartmental analysis of concentration–time data. Geometric mean values (% coefficient of variation) except mean body weight and $t_{1/2}$ (plus or minus standard deviation) and median T_{max} (range).
[a]Period B dosing: abrocitinib, 200 mg, orally, followed by an intravenous dose of ^{14}C-abrocitinib (5 minutes infusion) at ≈1 hour after oral dose.
[b]$\%F = 100\% \times (AUC_{po}/AUC_{iv}) \times (Dose_{iv}/Dose_{po})$.
[c]$\%f_af_g = 100\% \times (\text{Total } ^{14}C_{po}/\text{Total } ^{14}C_{iv})$.
CI, confidence interval; CL, clearance; V_{ss}, steady-state volume of distribution.

Plasma Protein Binding

An equilibrium dialysis method was used to determine plasma fraction unbound (f_u) values as described previously (Riccardi et al., 2017). Briefly, dialysis membranes (MWCO 12-14K) and 96-well dialysis devices were assembled following the manufacturer's instructions (HTDialysis, LLC, Gales Ferry, CT). Human plasma samples (pooled mixed sex; BioIVT, www.bioivt.com) containing 1 μM test compounds with 1% DMSO were dialyzed against PBS for 6 hours in a humidified incubator (75% relative humidity; 5% CO_2/95% air) at 37°C with shaking at 450 RPM. Quadruplicates of binding were measured for each compound. Samples were matrix-matched and quenched with cold acetonitrile-containing internal standard(s). The solutions were centrifuged (3600*g*, 30 minutes, 4°C), and the supernatant was analyzed using a generic LC-MS/MS method (Supplemental Tables 9–11).

Blood-to-Plasma Ratio

Human blood-to-plasma ratio was measured by Unilabs York Bioanalytical Solutions (York, UK). Test compounds were incubated in quadruplicate with fresh human blood (mixed sex, at least 1 sample per sex, Clinical Trials Laboratory Services Ltd, London, UK) at 1 μM in a humidified incubator (95% relative humidity; 5% CO_2/95% air) for 1 and 3 hours at 37°C with shaking at 450 RPM. Following incubation, plasma samples were obtained by centrifuging blood samples (3000*g*, 7 minutes). Both plasma and blood samples were matrix-matched with each other and quenched with acetonitrile-containing internal standard. The solutions were centrifuged, and the supernatant was analyzed using a generic LC-MS/MS method (Supplemental Tables 9–11). Peak area ratios were used to calculate blood-to-plasma ratio.

Results

Clinical Safety. All 6 participants completed the study. Oral and intravenous doses of abrocitinib in period A and B were safe and well tolerated, and no serious or drug-related adverse events were reported. All reported adverse events were mild in severity (Supplemental Table 12), and there were no clinically relevant changes in vital signs, clinical laboratory test results, or electrocardiogram measurements throughout the study period.

Pharmacokinetics. Plasma concentration-time profiles and pharmacokinetic parameters of abrocitinib are summarized in Fig. 1 and Table 1,

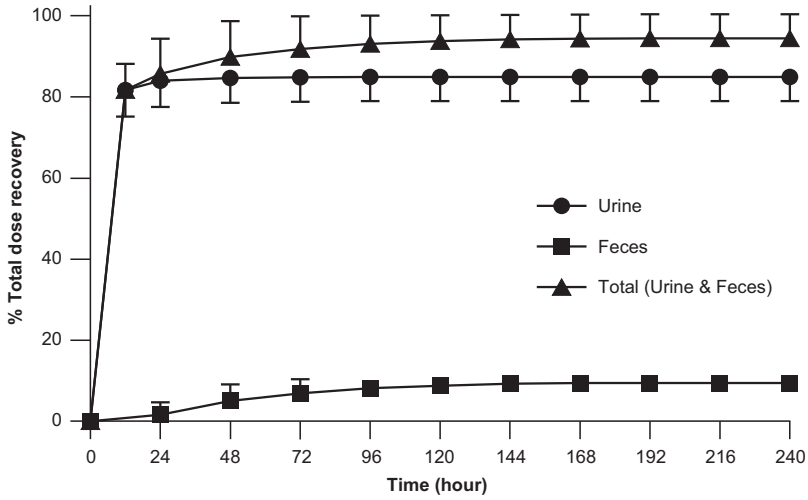

Fig. 2. Cumulative mean (plus or minus standard deviation) recovery of administered radioactivity in urine (85.0% ± 6.0%) and feces (9.5% ± 0.5%) following a single oral dose of 200 mg ^{14}C-abrocitinib (n = 6). Total recovery was 94.5% ± 5.9%.

respectively. Abrocitinib showed rapid absorption following oral administration, with a T_{max} of 0.5 hour. Systemic clearance and volume of distribution of abrocitinib were estimated at 64.2 L/h and 100 L, respectively. The absorption and elimination profiles of total radioactivity were comparable to those of abrocitinib, with >97% of circulating radioactivity measured within the 0- to 12-hour collection pool. There were some differences in P450 genotypes, with 3 participants with 2C19*1/*1 [extensive metabolizer (EM)] and 2C9*1/*1 (EM); 2 participants with 2C19*1/*17 (rapid metabolizer) and 2C9*1/*2 (intermediate metabolizer); and 1 participant with 2C19*1/*17 (rapid metabolizer) and 2C9*1/*1 (EM). However, these differences did not translate into significant differences in systemic clearance as percentage coefficient of variation was only 14%.

Disposition and Metabolite Profiles. After a single oral dose of ^{14}C-abrocitinib in male participants, radioactivity was excreted predominantly in the urine (Fig. 2). At 240 hours after the dose, the mean (plus or minus standard deviation) cumulative excretion in the urine was 85.0% (± 6.0%) and in the feces was 9.5% (± 0.5%) (Table 2). In total, 94.5% (± 5.9%) of the radioactive dose was recovered in urine and feces, with a major portion of excreted radioactivity recovered during the first 24 hours after dosing [urine 84.0% (± 6.4%), feces 1.7% (± 3.0%), total 85.7% (± 8.7%)]. Collectively, 13 metabolites were identified in urine and feces (Table 2). Oxidative metabolites M6, M1, M2, and M4 were the most abundant in urine at 12.2%, 16.2%, 13.5%, and 15.4% of the administered dose, respectively. All other metabolites comprised less than 10% of the dose. Representative HPLC radiochromatograms of plasma (0- to 12-hour pool after dose, representing >97% radioactivity AUC), urine (0- to 12-hour pool after dose, representing 96% of urine total recovery), and fecal (pools representing 97% of the feces total recovery) profiling are shown in Fig. 3. Unchanged abrocitinib accounted for the majority (25.8%) of the total circulating radioactivity (Table 2), with M1, M2, and M4 contributing 11.3%, 12.4%, and 13.8%, respectively. All remaining circulating metabolites made up less than 10% each of total circulating radioactivity.

Metabolite Identification. Structural determination was performed on 13 metabolites of abrocitinib. Metabolites were identified by comparing retention times on chromatograms and mass spectra of authentic standards or elucidated based on mass fragmentation patterns (Table 3; Supplemental Table 13). The proposed metabolic pathways of abrocitinib are shown in Fig. 4.

The parent compound, abrocitinib, had a retention time of 11.5 minutes using the HPLC conditions described. Abrocitinib has a protonated molecular ion at m/z 324.1490 (molecular formula $C_{14}H_{21}N_5O_2S$, theoretical mass m/z 324.1489). Its MS/MS spectrum showed diagnostic fragment ions at m/z 201, 176, 175, 149, and 70. The ion at

TABLE 2

Abrocitinib and metabolites in pooled plasma, urine, and feces samples following a single oral dose of 200 mg ^{14}C-abrocitinib (period A, n = 6)

Analyte	Plasma (% of Total Radioactivity)	Urine[b] (% of Dose)	Feces[b] (% of Dose)	Total Urine/Feces (% of Dose)
Abrocitinib	25.8	0.6	0.3	0.9
M4	13.8	15.4	0.3	15.7
M2[a]	12.4	13.5	0.5	14.0
M1	11.3	16.2	1.7	17.9
M3[a]	4.8	4.5	0.3	4.8
M7	4.6	5.6	1.5	7.1
M6	3.4	12.2	0.8	13.0
372-1	2.5	0.7	0.2	0.9
358-1	2.0	1.1	0.1	1.2
356-1a	1.5	1.7	0.2	1.9
356-2	1.5	3.3	0.6	3.9
M8	1.4	1.3	nd	1.3
340-5	1.0	0.4	0.2	0.6
M5	0.4	0.3	nd	0.3

Identified analytes ordered in relationship to prevalence in plasma.
nd, not detected.
[a]M2 and M3 are stereoisomers.
[b]Only percentages of identified metabolites are reported.

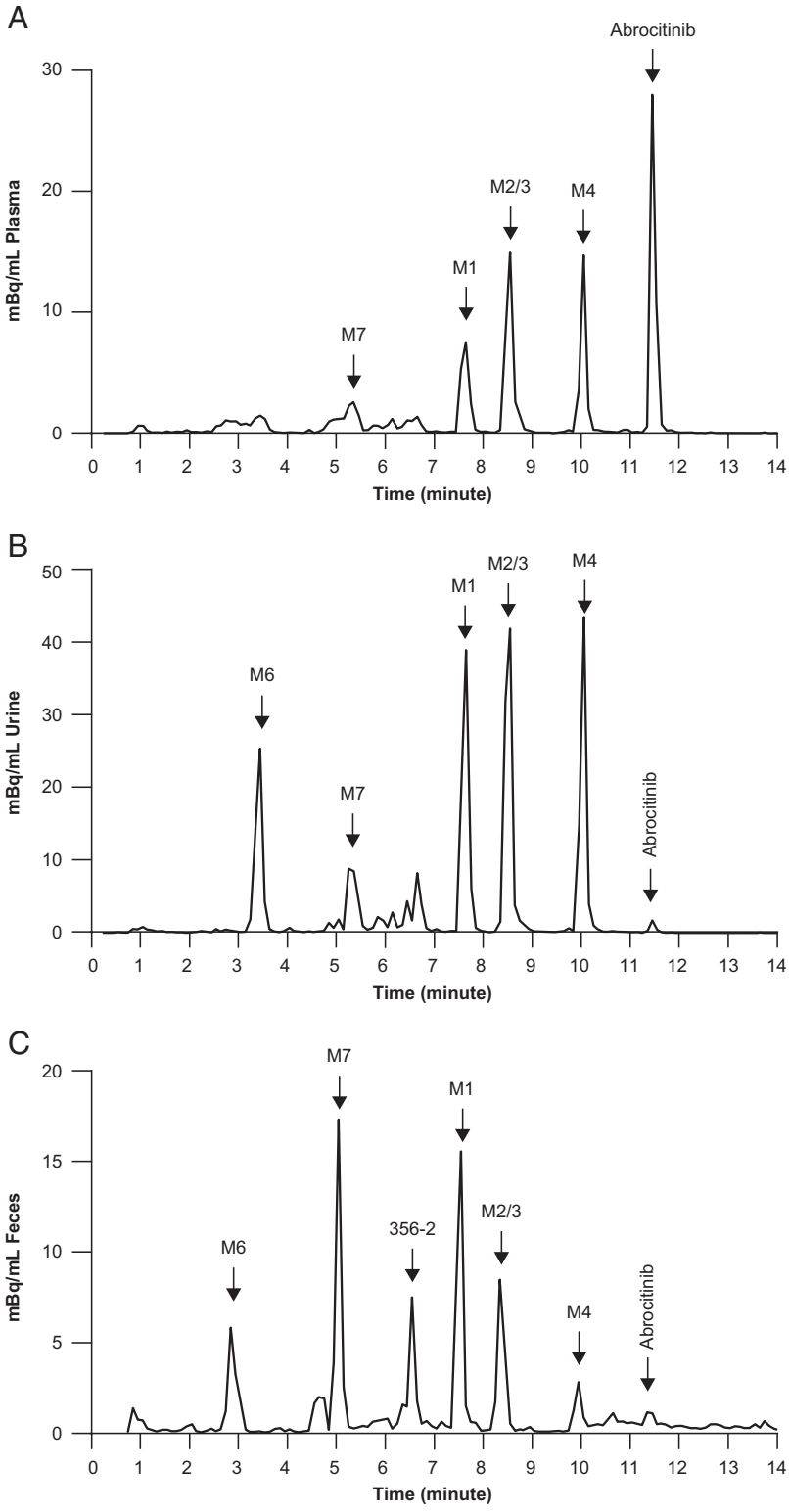

Fig. 3. Representative HPLC radiochromatograms of plasma (A), urine (B), and feces (C) following a single 200 mg dose of ^{14}C-abrocitinib.

m/z 201 resulted from the neutral loss of the propane-1-sulfonamide. Fragment m/z 176 represented the N-cyclobutylpropane-1-sulfonamide. Fragmentation through the cyclobutane ring yielded m/z 175. Fragment m/z 149, N-methyl-7H-pyrrolo[2,3- d]pyrimidin-4-amine, resulted from the neutral loss of N-cyclobutylpropane-1-sulfonamide, whereas fragment m/z 70 represented the cyclobutanamine ion.

Metabolite M6. M6 is a minor metabolite in plasma (3.4% of the radioactivity in the circulation) and was identified in urine (14.7%) and in fecal homogenate (8.3%) from profiled radioactivity. The amount of dose excreted as M6 in urine and fecal homogenate was 12.2% and 0.8%, respectively. M6 (molecular formula $C_{14}H_{19}N_5O_5S$, theoretical mass m/z 370.1180, observed mass m/z 370.1179) was 46 mass units

TABLE 3

Molecular ions and characteristic fragment ions of abrocitinib and metabolites detected in plasma and excreta

ID	Standard ID	Retention Time (min)	$[M+H]^+$ m/z	Parent Fragments m/z	Diagnostic Fragments m/z
M6	PF-07095462	3.4	370.1179	70	217, 165
340-5		4.9	340.1074	201, 176, 175, 149, 70	296
372-1		5.0	372.1334	176, 70	
M7	PF-06737821	5.2	354.1230	201, 175, 149, 70	218
M8	PF-07055039	5.8	356.1387	70	217, 165
358-1		6.1	358.1543	176, 70	235, 217, 183, 165
356-1a		6.4	356.1386	70	217, 192, 191, 165
356-2		6.5	356.1384	176, 70	233, 207, 181
M1	PF-06471658	7.6	340.1438	201, 175, 149, 70	218
M2	PF-07055087	8.5[a]	340.1438	201, 175, 149, 70	218
M3	PF-07055090	8.5[a]	340.1438	201, 175, 149, 70	218
M4	PF-07054874	10.0[b]	340.1438	176, 70	234, 217, 191, 165
M5	PF-07054926	10.0[b]	310.1332	176, 70	204, 187, 161, 135
Abrocitinib	PF-04965842	11.5	324.1490	201, 176, 175, 149, 70	

[a]Coeluting enantiomers followed by a second chromatographic separation (see *Methods*).
[b]Coeluting peaks with subsequent identification from urine isolation and nuclear magnetic resonance analyses (see *Methods*).

greater than parent and had a retention time of 3.4 minutes on HPLC. Fragmentation of the molecular ion yielded m/z 217, 165, and 70. Fragment m/z 217 represented the neutral loss of propane-1-sulfonamide and the addition of 16 mass units to the N-cyclobutyl-N-methyl-7H-pyrrolo[2,3-day]pyrimidin-4-amine. Fragment m/z 70, cyclobutanamine, remained intact. The remaining increase of 30 mass units was suggested to occur on the propane through di-oxidation and reduction.

NMR analysis of M6 (Supplemental Fig. 1) isolated from pooled 0- to 12-hour human urine supported formation of a carboxylic acid on the methyl group of the propyl side chain; it also supported formation of an amide carbonyl and a methylene at the 6' and 5′ positions of the pyrrolo pyrimidine ring, respectively. The methyl group was absent in the 1H spectrum of M6; in the homonuclear correlation spectroscopy (COSY) spectrum, cross peaks were observed between positions H18 (δ = 3.07 ppm) and H21 (δ = 2.31 ppm). Formation of the acid was further confirmed in the Heteronuclear Multiple Bond Correlation (HMBC) spectrum, which revealed cross peaks from both H18 and H21 into a carbon with a chemical shift value of 172.5 ppm, likely corresponding to the acid carbonyl (C22). Methines corresponding to the 6' and 5′ positions of the pyrrolo pyrimidine ring were both absent in the 1H spectrum of M6, and a new methylene at the 5′ position (1H/13C δ = 3.8/35.6 ppm) was observed. The HMBC spectrum revealed a cross peak between the newly formed methylene at the 5′ position (H9) into a carbon resonance at 175.2 ppm, suggesting the presence of an amide carbonyl at the 6' position (C8). Additional cross peaks in both COSY and HMBC spectra as well as resonances observed in the heteronuclear single quantum coherence spectrum (data not shown) indicated the rest of the molecule remained unmodified with respect to parent drug.

Metabolite 340-5. 340-5 was defined as a minor metabolite in plasma (1.0% of the radioactivity in the circulation). The amount of dose excreted as 340-5 in urine and fecal homogenate was 0.4% and 0.2%, respectively. The deformylated carboxylic acid metabolite, 340-5 (molecular formula $C_{13}H_{17}N_5O_4S$, theoretical mass m/z 340.1074, observed mass m/z 340.1074), was 16 mass units greater than parent and had a retention time of 4.9 minutes on HPLC. Fragmentation of the molecular ion yielded m/z 296, 218, 201, 175, 149, and 70. Fragment m/z 296 represented the neutral loss of 44 atomic mass units, which is diagnostic for the loss of COOH from the remaining ethane group. All other fragments were identical to the parent compound. Fragment m/z 218 represents the intact N-methyl-N-(7H-pyrrolo[2,3-day]pyrimidin-4-yl)cyclobutane-1,3-diamine portion of the molecule. All other fragments were identical to the parent compound.

Metabolite 372-1. 372-1 is a minor metabolite in plasma (2.5% of the radioactivity in the circulation). The amount of dose excreted as 372-1 in urine and fecal homogenate was 0.7% and 0.2%, respectively. The tri-hydroxylated metabolite, 372-1 (molecular formula $C_{14}H_{21}N_5O_5S$, theoretical mass m/z 372.1336, observed mass m/z 372.1334), was 48 mass units greater than parent and had a retention time of 5.0 minutes on HPLC. Fragmentation of the molecular ion yielded m/z 176 and 70. Fragment m/z 176 represented the intact N-cyclobutylpropane-1-sulfonamide, indicating that each oxidation was taking place on the N-methyl-7H-pyrrolo[2,3-day]pyrimidin-4-amine.

Metabolite M7. M7 was defined as a minor metabolite in plasma (4.6% of the radioactivity in the circulation). The amount of dose excreted as M7 in urine and fecal homogenate was 5.6% and 1.5%, respectively. The carboxylic metabolite, M7 (PF-06737821, 354-1) (molecular formula $C_{14}H_{19}N_5O_4S$, theoretical mass m/z 354.1231, observed mass m/z 354.1230), was 30 mass units greater than parent and had a retention time of 5.2 minutes on HPLC. Fragmentation of the molecular ion yielded m/z 218, 201, 175, 149, and 70. Fragment m/z 201 represented unchanged N-cyclobutyl-N-methyl-7H-pyrrolo[2,3-day]pyrimidin-4-amine.

NMR analysis of M7 (Supplemental Fig. 2) isolated from pooled 0- to 12-hour human urine supported formation of a carboxylic acid on the methyl group of the propyl side chain. The methyl group was absent in the 1H spectrum of 354-1, whereas in the COSY spectrum cross peaks were observed between positions H18 (δ = 3.12 ppm) and H21 (δ = 2.40 ppm). Formation of the acid was further confirmed in the HMBC spectrum, which revealed cross peaks from both H18 and H21 into a carbon with a chemical shift value of 172.5 ppm, likely corresponding to the acid carbonyl (C22). Additional cross peaks in both COSY and HMBC spectra as well as resonances observed in the heteronuclear single quantum coherence spectrum (data not shown) indicated the rest of the molecule remained unmodified with respect to parent drug.

Metabolite M8. M8 is a minor metabolite in plasma (1.4% of the radioactivity in the circulation). The amount of dose excreted as M8 in urine was 1.3%. The di-hydroxylated metabolite, M8 (PF-07055039, 356-1) (molecular formula $C_{14}H_{21}N_5O_4S$, theoretical mass m/z 356.1387, observed mass m/z 356.1387), was 32 mass units greater than parent and had a retention time of 5.8 minutes on HPLC. Fragmentation of the molecular ion yielded m/z 217, 165, and 70, which represented the proposed hydroxylation of the 7H-pyrrolo[2,3-day]pyrimidin-4-ylium group. The remaining hydroxylation was proposed to be located on the propyl group. Fragmentation was identical to the synthetic reference standard.

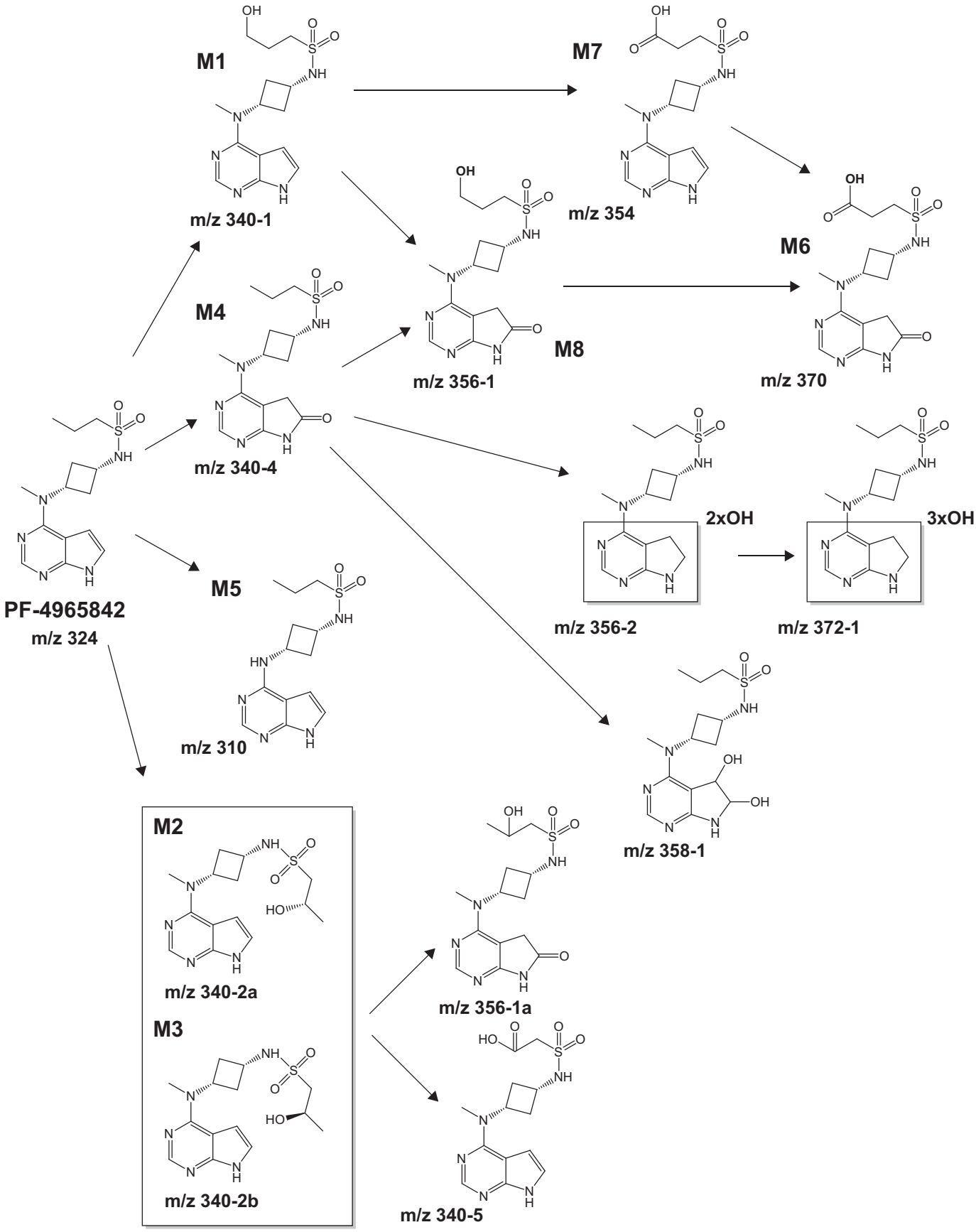

Fig. 4. Proposed metabolic pathways of abrocitinib following oral administration.

TABLE 4

f_{CL} by metabolite determined from abrocitinib incubation in human hepatocytes

Parameter	M1	M7	M2/M3	M4	358-1	372-1	149	Abrocitinib
% radioactivity	5.6	0.35	4.2	3.6	0.16	0.16	0.42	85
Metabolite f_{CL}	0.39	0.024	0.29	0.25	0.011	0.011	0.029	—
Final f_{CL}	0.41		0.29		0.27		0.029	—

Metabolite 358-1. 358-1 was defined as a minor metabolite in plasma (2.0% of the radioactivity in the circulation). The amount of dose excreted as 358-1 in urine and fecal homogenate was 1.1% and 0.1%, respectively. 358-1 (molecular formula $C_{14}H_{23}N_5O_4S$, theoretical mass m/z 358.1544, observed mass m/z 358.1543) was 34 mass units greater than parent, which represented the result of hydroxylation and hydrolysis. It had a retention time of 6.1 minutes on HPLC. Fragmentation of the molecular ion yielded m/z 217, 176, 165, and 70. Fragment m/z 176 represented the intact N-cyclobutylpropane-1-sulfonamide. Fragment m/z 183 represented the N-methyl-7Hpyrrolo [2,3-day]pyrimidin-4-amine with the addition of 34 mass units. The ions m/z 217 and 165 represented the loss of water and dehydration with the intact hydroxyl group on the 7H-pyrrolo[2,3-day]pyrimidin-4-ylium group.

Metabolite 356-1a. 356-1a was defined as a minor metabolite in plasma (1.5% of the radioactivity in the circulation). The amount of dose excreted as 356-1a in urine and fecal homogenate was 1.7% and 0.2%, respectively. The di-hydroxylated metabolite, 356-1a (molecular formula $C_{14}H_{21}N_5O_4S$, theoretical mass m/z 356.1387, observed mass m/z 356.1386), was 32 mass units greater than parent and had a retention time of 6.4 minutes on HPLC. Fragmentation of the molecular ion yielded m/z 217, 191, 165, and 70. The ion m/z 165 represented the proposed hydroxylation of the 7H-pyrrolo[2,3-day]pyrimidin-4-ylium group. The ion m/z 192 represented the proposed hydroxylation of the N-cyclobutylpropane-1-sulfonamide group.

Metabolite 356-2. 356-2 was defined as a minor metabolite in plasma (1.5% of the radioactivity in the circulation). The amount of dose excreted as 356-2 in urine and fecal homogenate was 3.3% and 0.6%, respectively. The di-hydroxylated metabolite, 356-2 (molecular formula $C_{14}H_{21}N_5O_4S$, theoretical mass m/z 356.1387, observed mass m/z 356.1385), was 32 mass units greater than parent and had a retention time of 6.5 minutes on HPLC. Fragmentation of the molecular ion yielded m/z 233, 207, 181, and 70. The ions m/z 233 and 181 represented the proposed di-hydroxylation of the 7H-pyrrolo[2,3-day]pyrimidin-4-ylium group.

Metabolite M1. M1 was defined as a major metabolite in plasma (11.3% of the radioactivity in the circulation). The amount of dose excreted as M1 in urine and fecal homogenate, was 16.2% and 1.7%, respectively. The hydroxylated metabolite, M1 (molecular formula $C_{14}H_{21}N_5O_3S$, theoretical mass m/z 340.1438, observed mass m/z 340.1438), was 16 mass units greater than parent and had a retention time of 7.6 minutes on HPLC. Fragmentation of the molecular ion yielded ions m/z 218, 175, 149, and 70, all identical to the parent molecule. Fragmentation was identical to the synthetic reference standard.

Metabolite M2. Both M2 and M3 are coeluting enantiomers. The abundance of the individual enantiomers was determined using both UHPLC and chiral chromatography. M2 was defined as a major metabolite in plasma (12.4% of the radioactivity in the circulation). The amount of dose excreted as M2 in urine and fecal homogenate was 13.5% and 0.5%, respectively. Hydroxylated M2 (molecular formula $C_{14}H_{21}N_5O_3S$, theoretical mass m/z 340.1438, observed mass m/z 340.1438) and M3 (molecular formula $C_{14}H_{21}N_5O_3S$, theoretical mass m/z 340.1438) are 16 mass units greater than parent. M2 had a retention time of 8.5 minutes on HPLC. Fragmentation of the molecular ion yielded ions m/z 201, 175, 149, and 70, which are all identical to the parent molecule. Fragmentation was identical to the synthetic reference standard.

Metabolite M3. M3 was defined as a minor metabolite in plasma (4.8% of the radioactivity in the circulation). The amount of dose excreted as M3 in urine and fecal homogenate was 4.5% and 0.3%, respectively. Fragmentation of the molecular ion yielded ions m/z 201, 175, 149, and 70, all identical to the parent molecule. Fragmentation was identical to the synthetic reference standard.

Metabolite M4. M4 was defined as a major metabolite in plasma (13.8% of the radioactivity in the circulation). The amount of dose excreted as M4 in urine and fecal homogenate was 15.4% and 0.3%, respectively. The oxidized metabolite, M4 (PF-07054874, 340-4), (molecular formula $C_{14}H_{21}N_5O_3S$, theoretical mass m/z 340.1438, observed mass m/z 340.1438) was 16 mass units greater than parent. This metabolite coeluted with M5. It had a retention time of 10.0 minutes on HPLC. Fragmentation of the molecular ion yielded m/z 217, 191, 176, 165, and 70. Fragmentation was identical to the synthetic reference standard.

Metabolite M5. M5 was defined as a minor metabolite in plasma (0.4% of the radioactivity in the circulation). The amount of dose excreted as M5 in urine was 0.3% and was not detected in fecal homogenate. The N-desmethylated metabolite, M5, (molecular formula $C_{13}H_{19}N_5O_2S$, theoretical mass m/z 310.1332, observed mass m/z 310.1332) was 14 mass units less than parent and had a retention time of 10.0 minutes on HPLC. This metabolite coeluted with M4. Fragmentation of the molecular ion yielded m/z 187, 161, and 135 (Table 3). Fragmentation was identical to the synthetic reference standard. The abundance of coeluting M4 and M5 were determined using the mass spectrometry, peak areas of reference standards at a single concentration. These peak

TABLE 5

Enzyme kinetic parameters of abrocitinib metabolism in human liver microsomes using Michaelis-Menten substrate inhibition modeling

Kinetic Parameter	M1	M2/M3	M4	Total
K_m, μM	143 ± 20	251 ± 26	519 ± 100	—
V_{max}, pmol/min per mg	26.7 ± 2.2	73.8 ± 5.0	881 ± 125	—
Ki, μM	1480 ± 316	1680 ± 320	1340 ± 430	—
CL_{int}, μL/min per mg	0.187	0.294	1.7	2.18
$CL_{int,app,sc}$, mL/min per kg	0.176	0.278	1.6	2.05
Fractional proportion $CL_{int,app,sc}$	0.086	0.136	0.780	

Data expressed as the mean plus or minus standard error of mean from triplicate replicates; unbound fraction ($f_{u,inc}$) of abrocitinib in human liver microsomes (0.3 mg/mL) was 1.
$f_{u,inc}$, unbound fraction; *Ki*, inhibition constant for substrates exhibiting substrate inhibition kinetics; V_{max}, maximum rate of metabolism.

TABLE 6

Selective P450 chemical inhibition of abrocitinib metabolism in pooled human hepatocytes and overall fractional P450 pathway assignment (f_m)

		% P450 Inhibition (Scaled)				P450 Pathway f_m			
Metabolite	f_{CL}	2B6	2C9	2C19	3A4	2B6	2C9	2C19	3A4
M1 (M7)	0.41	16	24	52	8.0	0.066	0.10	0.22	0.033
M2/M3	0.29		44	55			0.13	0.16	
M4 (358-1, 372-1)	0.27		25	57	18		0.067	0.15	0.048
149	0.029				100				0.030
		Overall f_m				0.066	0.30	0.53	0.11

Nonstatistical contributions by the remaining P450 isoforms for M1 (1A2, 2C8, 2D6), M2/M3 (1A2, 2B6, 2C8, 2D6, 3A), M4 (1A2, 2B6, 2C8, 2D6), and 149 (1A2, 2B6, 2C8, 2C9, 2C19, 2D6) were observed and excluded from fraction metabolized determinations. Fraction metabolized was calculated as the product of f_{CL} and fraction inhibited (scaled) as described in eq. 7.

areas were used to calibrate the abundance of M4 and M5 in the pooled plasma, urine, and feces sample extract profiles. The estimated mass ratio of M4 to M5 was determined to be 38.4, 49.4, and 13.3 for pooled plasma, urine, and fecal homogenate extracts, respectively. The combined [^{14}C] peak area for the pooled plasma extracts, pooled urine, and pooled fecal homogenate extracts was 14.2, 19.2, and 3.6%, respectively. The calculated individual contribution of [^{14}C] peak area for each metabolite (M4/M5) was 13.8/0.4% in pooled plasma extracts, 18.8/0.4% in pooled urine, and 3.3/0.3% in pooled fecal homogenate extracts.

P450 Phenotyping. The primary metabolites of abrocitinib were quantitated following a 30-minute incubation of ^{14}C-abrocitinib with human hepatocytes for determination of fractional contribution to total clearance. The resulting radiochromatogram is presented in Supplemental Fig. 3, and the percentage of total radioactivity associated with the formation of metabolites is presented in Table 4. Based on the percentage of total radioactivity observed at the 30-minute time point, the respective f_{CL} values were 0.390 for M1, 0.288 for M2/M3, 0.247 for M4, 0.0240 for M7, 0.011 for 358-1, 0.011 for 372-1, and 0.0291 for 149. Since M7 is likely a secondary metabolite of M1 (Fig. 4), the contribution of M7 metabolism was combined into the M1 route. Metabolites 358-1 and 372-1 are likely secondary metabolites of M4 (Fig. 4); therefore, the contributions were combined into the M4 route. The final f_{CL} values for the 4 metabolic pathways characterized were 0.414 for M1, 0.288 for M2/M3, 0.269 for M4, and 0.0291 for 149. The proportion of metabolism attributed to P450 activity from these 4 pathways totaled 1.0.

Enzyme kinetic parameters and intrinsic clearance values determined for the formation of M1, M2/M3, and M4 from abrocitinib metabolism in human liver microsomes are listed in Table 5, and associated data are presented graphically in Supplemental Fig. 4. Kinetic parameters for metabolite 149 could not be determined. Visual inspection of the Eadie-Hofstee plots for the M1, M2/M3, and M4 reaction rate data demonstrated nonlinear profiles consistent with substrate inhibition. For all 3 metabolites, a Michaelis-Menten equation with substrate inhibition was selected for the determination of enzyme kinetic parameters. Based on these kinetic parameters, the respective M1, M2/M3, and M4 $CL_{int,app}$ values were 0.187, 0.294, and 1.70 μL/min per mg and $CL_{int,app,sc}$ values were 0.176, 0.278, and 1.60 mL/min per kg. The total $CL_{int,app,sc}$ of three major metabolites for abrocitinib was 2.05 mL/min per kg.

The results of P450 selective chemical inhibition on the metabolism of abrocitinib in human hepatocytes are presented in Table 6. The metabolic formation rates of M1, M2/M3, and M4 were primarily inhibited in the presence of PPP (2B6), tienilic acid (2C9), esomeprazole (2C19), and troleandomycin (3A). After scaling, formation of metabolite M1 was inhibited 16% by PPP (2B6), 24% by tienilic acid, 52% by esomeprazole, and 8.0% by troleandomycin. Formation of metabolite M2/M3 was inhibited 45% by tienilic acid and 55% by esomeprazole. M4 was inhibited 25% by tienilic acid, 57% by esomeprazole, and 18% by troleandomycin. A summary of the abrocitinib P450 assignment is presented in Table 6. After normalizing for f_{CL} for each metabolic pathway, the fraction of metabolic clearance of abrocitinib catalyzed by CYP2C19, 2C9, 3A4, and 2B6 were 0.53, 0.30, 0.11, and 0.066, respectively.

In Vitro Pharmacology. The enzyme potency of abrocitinib and the oxidative metabolites M1, M2, and M4 was assessed against four JAK isoforms using enzymatic assays at 1 mM adenosine triphosphate (Table 7). Abrocitinib was more potent against JAK1 versus JAK2 or TYK2 and demonstrated little potency for JAK3 (IC_{50} >10,000 nM). M1 and M2 exhibited a similar potency and selectivity profile as abrocitinib. The IC_{50} values for M4 with all 4 JAK isoforms were >10,000 nM. Therefore, the circulating metabolites M1 and M2 are active metabolites that may contribute to the overall pharmacology of abrocitinib, whereas M4 is pharmacologically inactive.

The cellular potency of abrocitinib, M1, and M2 was evaluated by measuring the inhibition of phosphorylation of STATs following stimulation with various cytokines in human whole blood (represented as total and unbound IC_{50}), human keratinocytes, and THP-1 cells (IC_{50} values considered unbound) (Table 8). Abrocitinib was much more potent against cytokines that transduce their signals via JAK1-dependent pathways, with IC_{50} values ranging from 40.0 nM for IL-31–induced STAT3 phosphorylation to 1690 nM (unbound 569 nM) for interferon (IFN)-γ–induced STAT1 phosphorylation when compared with cytokines that transduce signals via JAK1-independent pathways, with IC_{50} values ranging from 7180 nM (unbound 2420 nM) for EPO-induced STAT5 phosphorylation to >16,500 nM (unbound >5550 nM) for IL-23–induced STAT3 phosphorylation. Like abrocitinib, M1 and M2 inhibited JAK1-dependent signaling pathways more potently than JAK1-independent signaling pathways. In addition, the relative selectivity or potency rank order across cytokine inhibition was similar between abrocitinib, M1, and M2.

The fraction unbound in plasma for each active drug species was determined to be 0.36 for abrocitinib, 0.63 for M1, and 0.71 for M2. The

TABLE 7

In vitro enzymatic potency of abrocitinib and human metabolites M1, M2, and M4

	IC_{50} (nM)[a]			
JAK Assay	Abrocitinib	M1	M2	M4
JAK1	29.2	43.4	17.9	>10,000
JAK2	803	1140	886	>10,000
JAK3	>10,000	>10,000	>10,000	>10,000
TYK2	1250	3190	1210	>10,000

[a]IC_{50} values obtained at 1 mM adenosine triphosphate.

TABLE 8

In vitro cellular potency of abrocitinib and human metabolites M1 and M2

Cytokine-Induced pSTAT Assay				$IC_{50}/IC_{50,u}$[a] (nM)		
Cytokine	JAK Pair	pSTAT	Cell Assay	Abrocitinib	M1	M2
IL-4	JAK1/JAK2	pSTAT6	Human keratinocytes	77.0	433	134
IL-13	JAK1/JAK2	pSTAT6	Human keratinocytes	81.9	236	84.1
IL-22	JAK1/TYK2	pSTAT3	Human keratinocytes	420	703	198
IL-31	JAK1/JAK2	pSTAT3	IFNγ-primed THP-1	40.0	79.6	56.0
TSLP	JAK1/JAK2	pSTAT3	hWB ($CD3^+$ cells)	1020/343	785/438	271/152
IFNα	JAK1/TYK2	pSTAT3	hWB (lymphocytes)	174/58.5	296/165	90.5/50.6
IFNγ	JAK1/JAK2	pSTAT1	hWB ($CD14^+$ cells)	1690/569	1950/1090	2160/1210
IL-6	JAK1/JAK2	pSTAT1	hWB ($CD3^+$ cells)	343/115	171/95.3	136/76.0
IL-12	JAK2/TYK2	pSTAT4	hWB (lymphocytes)	9730/3270	33,400/18,600	5170/2890
IL-15	JAK1/JAK3	pSTAT5	hWB (lymphocytes)	537/181	558/311	353/197
IL-21	JAK1/JAK3	pSTAT3	hWB (lymphocytes)	516/174	844/471	487/272
IL-23	JAK2/TYK2	pSTAT3	hWB (lymphocytes)	>16,500>5550	26,200/14,600	6210/3470
IL-27	JAK1/JAK2	pSTAT3	hWB (lymphocytes)	228/76.7	382/213	234/131
EPO	JAK2/JAK2	pSTAT5	hWB (spiked $CD34^+$ cells)	7180/2420	9750/5440	9470/5290

B/P, blood/plasma ratio; EPO, erythropoietin; hWB, human whole blood; $IC_{50,u}$, unbound IC_{50}; pSTAT, phospho-signal transducer and activator of transcription; TSLP, thymic stromal lymphopoietin.

[a]hWB $IC_{50}/IC_{50,u}$: total IC_{50}/unbound IC_{50}; unbound IC_{50} = hWB IC_{50} × (f_u/B/P ratio); abrocitinib f_u = 0.36; M1 f_u = 0.63; M2 f_u = 0.71; abrocitinib B/P = 1.07; M1 B/P = 1.13; M2 B/P = 1.27; mean IC_{50} from at least two experiments.

blood/plasma ratios for each drug species were determined to be 1.07 for abrocitinib, 1.13 for M1, and 1.27 for M2. Blood binding parameters were used to convert whole-blood pharmacology potency values into unbound values (Table 8).

Discussion

In this report, the pharmacokinetics and metabolism of abrocitinib were evaluated in healthy human participants. Recovery of the radiolabeled dose was ∼95%, indicating that the disposition of abrocitinib was well characterized. Oral absorption of abrocitinib was >90% and rapid, with peak concentrations observed at ∼0.5 hour, despite being identified as an MDR1 and BCRP efflux substrate. Absolute oral bioavailability was determined to be ∼60% and elimination half-life ($t_{1/2}$) ∼2 hour. Systemic clearance was observed to be 64.2 L/h, and steady-state volume of distribution was 100 L. Clinical experience with abrocitinib has shown dose-proportional oral pharmacokinetics over a range of 30–400 mg, which supports linearity of parent and metabolite profiles. The $t_{1/2}$ of both abrocitinib and total radioactivity profiles was similar, indicating formation rate limited kinetics of metabolites. Following a single oral dose of abrocitinib, the major circulating component of drug-related material in plasma was abrocitinib (∼26%), followed by three monohydroxylated metabolites (M1, M2, and M4) at >10%. However, following multiple daily dosing of abrocitinib to steady state, analytical measurement of metabolites indicated that M2 and M4 were observed at >10%, with M1 being considered minor at <10% (data on file).

Disposition profiles indicated oxidative metabolism as the major pathway of clearance for abrocitinib, whereas the renal route of elimination was minor at <1%. All the metabolites of abrocitinib were consistent with oxidative P450 metabolism, with no observed evidence of direct conjugative mechanisms. In vitro phenotyping indicated multiple P450 enzymes involved in the metabolism of abrocitinib, with hepatic fraction of metabolism (f_m) assignments of 0.53 for CYP2C19, 0.30 for

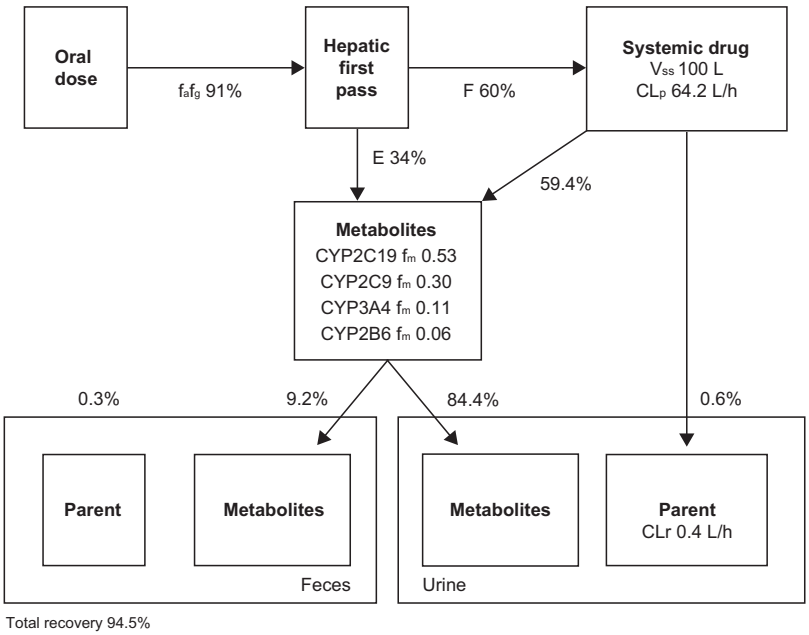

Fig. 5. Proposed mass balance model for abrocitinib following oral administration. CL_p, plasma clearance; CLr, renal clearance; F, bioavailability; f_af_g, fraction absorbed × fraction surviving gut metabolism; V_{ss}, steady state volume of distribution.

CYP2C9, 0.11 for CYP3A4, and ~0.06 for CYP2B6. These in vitro results are in agreement with the impact of strong CYP2C19 inhibition by fluvoxamine and fluconazole on the exposure of coadministered abrocitinib (Wang et al., 2022b). Collectively, a mass balance model was assembled for abrocitinib and is shown in Fig. 5.

In contrast to abrocitinib, renal elimination was observed as the major pathway of excretion for metabolites. The f_m of renal elimination was estimated to be 0.74 for M1, 0.94 for M2, and 0.93 for M4, based on clinical observation (Wang et al., 2022a). Active renal clearance was predicted to be >80% for each of the metabolites, with the balance from passive filtration (f_u × glomerular filtration rate), based on estimates of metabolite exposure in plasma and total amount excreted in urine (total renal clearance = mass in urine/AUC). In vitro profiling showed that each of the primary metabolites was a substrate for the OAT3 transporter (internal data). A clinical study with the OAT3 inhibitor probenecid and coadministered abrocitinib showed an AUC_{inf} increase of approximately twofold for each of the metabolites in plasma (M1, 1.8-fold; M2, 2.2-fold; M4, 2.2-fold) (Wang et al., 2022b).

Abrocitinib and its metabolites M1 and M2 were pharmacologically active at inhibiting cytokine signaling through JAK1 heterodimer pairs (i.e., JAK1/JAK2, JAK1/TYK2, and JAK1/JAK3), whereas M4 was inactive. The relative JAK selectivity was similar among abrocitinib, M1, and M2. Clinical assessment of the contribution of abrocitinib, M1, and M2 to circulating plasma pharmacology based on steady-state AUC and relative potency (Leclercq et al., 2009) indicated respective percentages of ~60%, ~10%, and ~30% (data on file). Dose adjustment of abrocitinib in the context of drug-drug interaction and in special populations (renal/hepatic impairment) will be based on the total contribution of abrocitinib, M1, and M2 pharmacology (i.e., total active moiety) (Wang et al., 2021; Wang et al., 2022a; Wang et al., 2022b).

In summary, these study results provide an important and comprehensive characterization of abrocitinib pharmacokinetics, metabolism, and clearance mechanisms as well as disposition and pharmacology of major metabolites. Furthermore, the disposition characterization of abrocitinib and its major metabolites has been consistent with clinical experience in drug-drug interaction studies and special populations.

Upon request, and subject to review, Pfizer will provide the data that support the findings of this study. Subject to certain criteria, conditions, and exceptions, Pfizer may also provide access to the related individual deidentified participant data. See https://www.pfizer.com/science/clinical-trials/trial-data-and-results for more information.

Clinicaltrials.gov identifier: NCT03250039.

Acknowledgments

The authors would like to thank Xin Yang for technical assistance associated with in vitro P450 phenotyping and Rianne A.F. de Ligt, Esther van Duijn, and Wouter Vaes from TNO for their contributions toward the metabolite profiling work. Editorial support under the guidance of authors was provided by Marianna Johnson at ApotheCom, San Francisco, CA, and was funded by Pfizer Inc., New York, NY, in accordance with Good Publication Practice (GPP3) guidelines (*Ann Intern Med.* 2015, 163:461–464).

Authorship Contributions

Participated in research design: Bauman, Doran, King-Ahmad, Sharma, Walker, J. Lin, T.H. Lin, Telliez, Tripathy, Goosen, Banfield, Malhotra, Dowty.

Conducted experiments: Bauman, Doran, King-Ahmad, Sharma, Walker, J. Lin, T.H. Lin, Telliez, Tripathy.

Performed data analysis: Bauman, Doran, King-Ahmad, Sharma, Walker, J. Lin, Tripathy, Goosen, Banfield, Dowty.

Wrote or contributed to the writing of the manuscript: Bauman, Doran, T.H. Lin, Tripathy, Goosen, Banfield, Dowty.

References

Akada H, Akada S, Hutchison RE, Sakamoto K, Wagner KU, and Mohi G (2014) Critical role of Jak2 in the maintenance and function of adult hematopoietic stem cells. *Stem Cells* **32**:1878–1889.

Bieber T, Simpson EL, Silverberg JI, Thaçi D, Paul C, Pink AE, Kataoka Y, Chu CY, DiBonaventura M, Rojo R, et al.; JADE COMPARE Investigators (2021) Abrocitinib versus Placebo or Dupilumab for Atopic Dermatitis. *N Engl J Med* **384**:1101–1112.

Dowty ME, Lin TH, Jesson MI, Hegen M, Martin DA, Katkade V, Menon S, and Telliez JB (2019) Janus kinase inhibitors for the treatment of rheumatoid arthritis demonstrate similar profiles of in vitro cytokine receptor inhibition. *Pharmacol Res Perspect* **7**:e00537.

Gooderham MJ, Forman SB, Bissonnette R, Beebe JS, Zhang W, Banfield C, Zhu L, Papacharalambous J, Vincent MS, and Peeva E (2019) Efficacy and Safety of Oral Janus Kinase 1 Inhibitor Abrocitinib for Patients With Atopic Dermatitis: A Phase 2 Randomized Clinical Trial. *JAMA Dermatol* **155**:1371–1379.

Hamilton RA, Garnett WR, and Kline BJ (1981) Determination of mean valproic acid serum level by assay of a single pooled sample. *Clin Pharmacol Ther* **29**:408–413.

Leclercq L, Cuyckens F, Mannens GSJ, de Vries R, Timmerman P, and Evans DC (2009) Which human metabolites have we MIST? Retrospective analysis, practical aspects, and perspectives for metabolite identification and quantification in pharmaceutical development. *Chem Res Toxicol* **22**:280–293.

Peeva E, Hodge MR, Kieras E, Vazquez ML, Goteti K, Tarabar SG, Alvey CW, and Banfield C (2018) Evaluation of a Janus kinase 1 inhibitor, PF-04965842, in healthy subjects: A phase 1, randomized, placebo-controlled, dose-escalation study. *Br J Clin Pharmacol* **84**:1776–1788.

Riccardi K, Lin J, Li Z, Niosi M, Ryu S, Hua W, Atkinson K, Kosa RE, Litchfield J, and Di L (2017) Novel method to predict in vivo liver-to-plasma K_{puu} for OATP substrates using suspension hepatocytes. *Drug Metab Dispos* **45**:576–580.

Silverberg JI, Simpson EL, Thyssen JP, Gooderham M, Chan G, Feeney C, Biswas P, Valdez H, DiBonaventura M, Nduaka C, et al. (2020) Efficacy and Safety of Abrocitinib in Patients With Moderate-to-Severe Atopic Dermatitis: A Randomized Clinical Trial. *JAMA Dermatol* **156**:863–873.

Simpson EL, Sinclair R, Forman S, Wollenberg A, Aschoff R, Cork M, Bieber T, Thyssen JP, Yosipovitch G, Flohr C, et al. (2020) Efficacy and safety of abrocitinib in adults and adolescents with moderate-to-severe atopic dermatitis (JADE MONO-1): a multicentre, double-blind, randomised, placebo-controlled, phase 3 trial. *Lancet* **396**:255–266.

Spracklin DK, Chen D, Bergman AJ, Callegari E, and Obach RS (2020) Mini-review: comprehensive drug disposition knowledge generated in the modern human radiolabeled ADME study. *CPT Pharmacometrics Syst Pharmacol* **9**:428–434.

Trier AM and Kim BS (2018) Cytokine modulation of atopic itch. *Curr Opin Immunol* **54**:7–12.

van Duijn E, Sandman H, Grossouw D, Mocking JA, Coulier L, and Vaes WHJ (2014) Automated combustion accelerator mass spectrometry for the analysis of biomedical samples in the low attomole range. *Anal Chem* **86**:7635–7641.

Walsky RL and Obach RS (2007) A comparison of 2-phenyl-2-(1-piperidinyl)propane (ppp), 1,1′,1′′-phosphinothioylidynetrisaziridine (thioTEPA), clopidogrel, and ticlopidine as selective inactivators of human cytochrome P450 2B6. *Drug Metab Dispos* **35**:2053–2059.

WangEQ, Le V, O'Gorman M, Tripathy S, Dowty ME, Wang L, and Malhotra BK (2021) Effects of hepatic impairment on the pharmacokinetics of abrocitinib and its metabolites. *J Clin Pharmacol* **61**:1311–1323.

Wang EQ, Le V, Winton JA, Tripathy S, Raje S, Wang L, Dowty ME, and Malhotra BK (2022a) Effects of Renal Impairment on the Pharmacokinetics of Abrocitinib and Its Metabolites. *J Clin Pharmacol* **62**:505–519.

Wang X, Dowty ME, Wouters A, Tatulych S, Connell CA, Le VH, Tripathy S, O'Gorman MT, Winton JA, Yin N, et al. (2022b) Assessment of the effects of inhibition or induction of CYP2C19 and CYP2C9 enzymes, or inhibition of OAT3, on the pharmacokinetics of abrocitinib and its metabolites in healthy individuals. *Eur J Drug Metab Pharmacokinet* **47**:419–429.

Yang X, Atkinson K, and Di L (2016) Novel cytochrome P450 reaction phenotyping for low-clearance compounds using the hepatocyte relay method. *Drug Metab Dispos* **44**:460–465.

Address correspondence to: Martin E. Dowty, Pfizer Inc., 1 Portland St, Cambridge, MA 02139. E-mail: martin.dowty@pfizer.com